Available online at www.sciencedirect.com
SCIENCE DIRECT®
Journal of Molecular Spectroscopy 227 (2004) 13–22
Journal of MOLECULAR SPECTROSCOPY
www.elsevier.com/locate/jms

Part of the far-infrared laser magnetic resonance spectrum of the HF^+ free radical

Michael D. Allen,[a,1] Kenneth M. Evenson,[a,2] and John M. Brown[b,*]

[a] *Time and Frequency Division, NIST, 325 Broadway, Boulder, CO 80303, USA*
[b] *The Physical and Theoretical Chemistry Laboratory, The Chemistry Department, South Parks Road, Oxford OX1 3QZ, UK*

Received 1 April 2004
Available online 2 June 2004

Abstract

Transitions between the spin-rotational levels of the HF^+ radical in the $v = 0$ level of the $X^2\Pi$ ground state have been observed by the technique of laser magnetic resonance at far-infrared wavelengths. Because of the large spin–orbit coupling in this $^2\Pi$ state, the detection of the fine-structure transitions required the use of very short-wavelength laser lines (down to 40 μm). These observations have provided accurate information on the ^{19}F hyperfine splittings in rotational levels of the upper $^2\Pi_{1/2}$ spin component for the first time which has enabled the complete determination of the hyperfine structure for this molecule. An effective Hamiltonian was used to model the experimental measurements; this provided considerably more accurate values for the various molecular parameters than previously available. Using these parameters, predictions of the transition frequencies between the low-lying spin-rotational levels of the radical at zero magnetic field have been made.

1. Introduction

The HF^+ radical is iso-electronic with OH (and also NH^-). It therefore comes as something of a surprize to discover that it has been comparatively little studied by spectroscopists. Frost et al. [1] were the first to observe the molecule, using photoelectron spectroscopy of HF. These results were improved upon and corrected soon afterwards by Brundle [2]. He was able to determine the vertical ionization energies to the $X^2\Pi$ ground and $A^2\Sigma^+$ excited states of HF^+ and the approximate vibrational intervals in these states. These values were further refined in subsequent photo-ionization [3] and photoelectron [4] experiments at higher resolution; it was even possible to resolve the spin–orbit splitting in the $X^2\Pi$ state by detecting the threshold electrons [5]. At about the same time, Gewurtz et al. [6] recorded the emission spectrum associated with the weak $A^2\Sigma^+$–$X^2\Pi$ electronic transition at rotational resolution. They determined values for many of the important properties of the ion, including the dissociation limit of the weakly bound $A^2\Sigma^+$ state. A few years later, part of the rotational spectrum of HF^+ in the ground state was recorded by Hovde et al. [7] using the technique of laser magnetic resonance (LMR) at far-infrared wavelengths. This study revealed the rather large hyperfine splittings associated with the ^{19}F nucleus for the first time but was restricted to a single rotational transition in the lower $^2\Pi_{3/2}$ spin component. The final piece of experimental information on HF^+ was provided by Hovde et al. [8] who recorded some *R*-lines in the fundamental band of the vibration–rotation spectrum at about 2912 cm^{-1}; they used velocity modulation to detect the signals. This produced a more accurate measurement of the vibrational interval and also revealed ^{19}F hyperfine structure on some of the lower-*J* transitions.

HF^+ has also been the subject of some theoretical calculations. These have been concerned with the electronic structure of the molecule in its lowest electronic states [9,10], the lambda-doubling intervals [11,12], and nuclear hyperfine structure [13]; both the latter refer to the molecule in the $X^2\Pi$ state.

* Corresponding author. Fax: +44-1865-275410.
E-mail address: jmb@physchem.ox.ac.uk (J.M. Brown).
[1] Present address: Xilinx, 3100 Logic Drive, Longmont, CO 80503, USA.
[2] Ken Evenson died on 29 January 2002.

0022-2852/$ - see front matter © 2004 Elsevier Inc. All rights reserved.
doi:10.1016/j.jms.2004.05.001

The major advance in far-infrared spectroscopy in recent years has been a push to shorter wavelengths, into the "true" far-infrared region below 100 μm. This has enabled the detection of pure rotational transitions of very light molecules [14], fine-structure transitions in both atoms [15] and molecules [16] and even some vibration–rotation transitions for low-frequency bending vibrations [17]. One limitation of the earlier high resolution studies of HF^+ in the $X^2\Pi$ state was that they provided rather little information on the molecule in the upper, $^2\Pi_{1/2}$ spin component. These levels lie some 310 cm^{-1} above those of the lower component and are by comparison rather sparsely populated. In addition, the molecule has a very small magnetic moment in these upper levels which hinders their study by magnetic resonance methods. Information on the $^2\Pi_{1/2}$ levels is needed for a complete determination of the molecular parameters of HF^+ (for example, there are four hyperfine parameters for each nucleus but studies of the $^2\Pi_{3/2}$ levels give direct information on only one of them). The availability of new, short-wavelength far-infrared laser lines brings the fine-structure transitions of HF^+ into range and so gives access to these levels.

In this paper, we report a limited study of the fine-structure transitions of HF^+ in the $v = 0$ level of the $X^2\Pi$ state by LMR together with an extension of the pure rotational transitions in the $^2\Pi_{3/2}$ component. These measurements are sufficient to provide a complete determination of the molecular parameters for this molecule with a considerable improvement in accuracy. The bond length of the molecule has been refined as a result. The ^{19}F hyperfine parameters obtained make an interesting comparison with those predicted by theory [13].

2. Experimental details

The far-infrared LMR experiments were performed at the Boulder laboratories of NIST; the spectrometer has been described in detail elsewhere [18]. The HF^+ radicals were produced in the spectrometer sample volume by flowing a lean mixture of HF in helium through a special microwave discharge designed so that the resultant plasma projected out into the laser radiation field. A similar microwave discharge source has been described briefly in our earlier study of OH^+ [19]. The total pressure in the sample volume was about 0.4 Torr (55 Pa). The HF gas was dried with liquid nitrogen and bled into the discharge at a rate which did not register on the pressure gauge (less than 2 mTorr). The far-infrared radiation was coupled out of the laser cavity and detected with a liquid helium-cooled gallium–germanium photo-conductor. The magnetic field was modulated at a frequency of 39 kHz and the signal detected with a lock-in amplifier at the same frequency. The resonances were consequently displayed as the first derivative of an absorption profile. The magnet of the LMR system was controlled by a rotating-coil magnetometer which provided a direct readout of the flux densities. The system was calibrated periodically up to 1.8 T with a proton NMR gaussmeter; the absolute uncertainty of measurement was 10^{-5} T below 0.1 T and the fractional uncertainty was 10^{-4} above 0.1 T.

3. Results and analysis

3.1. Observations and assignments

The far-infrared transitions of HF^+ in the $v = 0$ level which have been detected in the LMR experiment are summarized in Table 1; they are also shown on the energy level diagram in Fig. 1. All together, resonances associated with five separate rotational and fine-structure transitions have been observed. An example from the 87.73 μm spectrum is shown in Fig. 2; the transition involved is $J = 7/2 \leftarrow 5/2$, $M_J = -3/2 \leftarrow -5/2$ in the $^2\Pi_{3/2}$ component. The ^1H nuclear hyperfine interaction is responsible for the small doubling of each line in this spectrum while the corresponding interaction involving the ^{19}F nucleus produces a much larger doublet splitting of about 100 mT (both nuclei have $I = 1/2$). A second example in Fig. 3 shows a single Zeeman component of the $J = 5/2 \leftarrow 7/2$ fine-structure transition, recorded with the 44.24 μm line. The HF^+ resonance corresponds

Table 1
Summary of observations in the far-infrared LMR spectrum of HF^+ in the $v = 0$ level of its $X^2\Pi$ state

HF^+ transitions observed			Laser line			
Ω	J	Parity	λ (μm)	ν (GHz)	Gas	Pump
Rotational transitions						
3/2	5/2–3/2	$\mp \leftarrow \pm$	124.4	2409.2933	CH_2DOH	10P(34)
			122.5	2447.9685	CH_2F_2	9R(22)
	7/2–5/2	$\pm \leftarrow \mp$	87.73	3417.2639	CD_3OD	10P(38)
Fine-structure transitions						
1/2–3/2	7/2–9/2	$- \leftarrow +$	48.72	6153.2790	CD_3OH	9R(6)
	5/2–7/2	$\mp \leftarrow \pm$	44.24	6775.7835	CH_3OH	9P(16)
	3/2–5/2	$\pm \leftarrow \mp$	39.92	7509.0362	CH_3OH	9P(34)

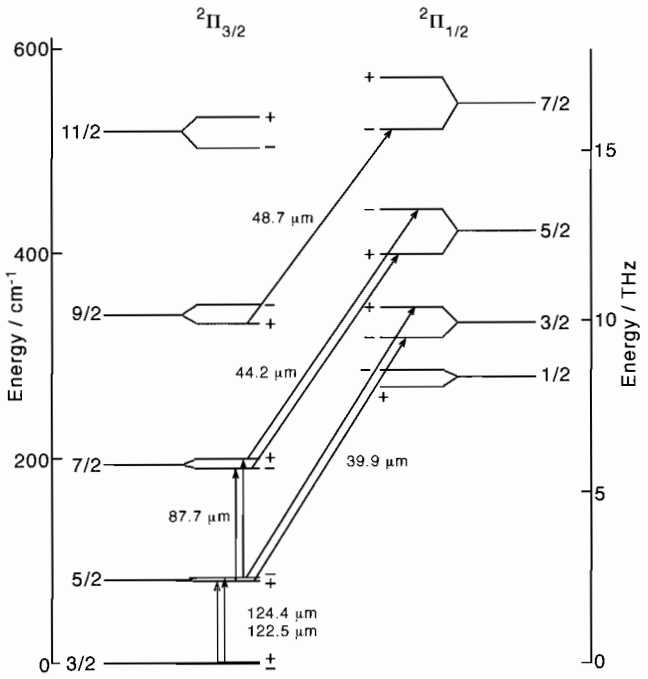

Fig. 1. Diagram showing the lower energy levels of the HF^+ radical in the $v = 0$ level of the $X^2\Pi$ state and the transitions involved in the observed far-infrared LMR spectrum. The lambda-type (parity) doubling has been exaggerated by a factor of 20 for the sake of clarity.

to one of the two ^{19}F hyperfine doublets; its companion lies to higher field beyond the end of the region shown. The line shows a just resolvable ^1H doubling when recorded more slowly over a narrower field range. It can be seen by comparison of Fig. 3 with 2 that the fine-structure transitions (which are electric-dipole in character) are much weaker than the pure rotational transitions. The spectra recorded with short-wavelength laser lines all show the presence of several "impurity" species in the discharge, despite the simplicity of the production method. One of these is, of course, the OH radical in its $X^2\Pi$ state. It produces strong signals on the 124.4 μm line ($J = 5/2 \leftarrow 3/2$ in the $^2\Pi_{3/2}$ component of the $v = 1$ level), the 87.73 μm line ($J = 7/2 \leftarrow 5/2$ in the $^2\Pi_{3/2}$ component of the $v = 1$ level), and the 48.72 μm line ($J = 7/2 \leftarrow 9/2$, $^2\Pi_{1/2}$–$^2\Pi_{3/2}$ fine-structure transition in the $v = 0$ level). Part of the 87.73 μm spectrum is shown in Fig. 2. Several unidentified signals remain. Three are shown in Fig. 3 where it can be seen that some of them are very strong. The two signals marked B appear to be related. If the splitting of 180 mT between them corresponds to a hyperfine interaction, it strongly suggests that the molecule concerned contains a fluorine atom. Further investigation of these intriguing observations is being undertaken.

The detailed measurements of the individual resonances for the six laser lines used to record LMR spectra are given in Table 2. The assignments were made with the help of a computer program which predicts all possible resonances for a given laser frequency, together with their lines strengths and tuning rates [20,21]. This information constitutes the Zeeman pattern which can be used to make the assignments even when the

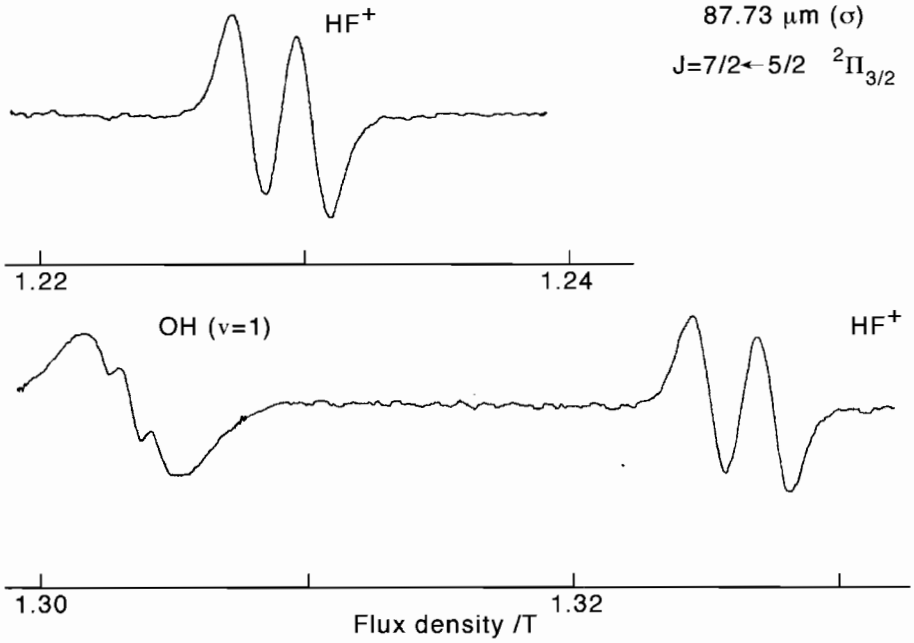

Fig. 2. Part of the far-infrared LMR spectrum of the HF^+ radical in the $v = 0$ level of the $X^2\Pi$ state. The spectrum is recorded with the 87.73 μm laser line in perpendicular polarization ($\Delta M_J = \pm 1$). The rotational transition involved is $J = 7/2 \leftarrow 5/2$, $\Omega = 3/2$, $M_J = -3/2 \leftarrow -5/2, + \leftarrow -$. The ^{19}F and ^1H hyperfine structures are both fully resolved; the nuclear spin selection rule is $\Delta M_I = 0$ (see Table 2). This scan also shows one of the OH impurity lines resulting from the microwave discharge through (slightly damp) HF in helium. In this case, the OH is vibrationally excited, in the $v = 1$ level.

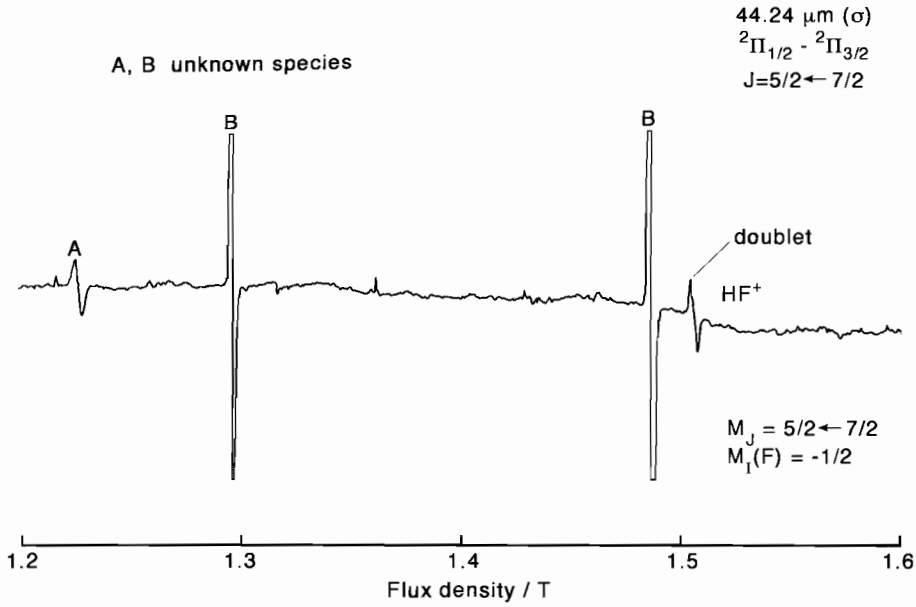

Fig. 3. Part of the far-infrared LMR spectrum of the HF^+ radical in the $v = 0$ level of the $X^2\Pi$ state, recorded with the 44.24 μm laser line in perpendicular polarization ($\Delta M_J = \pm 1$). The transition involved is a fine-structure transition with $J = 5/2 \leftarrow 7/2, - \leftarrow +, M_J = 5/2 \leftarrow 7/2$. Note that this signal is much weaker than the pure rotational transitions shown in Fig. 2. The ^{19}F hyperfine splitting is fully resolved; the other hyperfine component lies at higher flux densities, beyond the range of this scan. The ^1H hyperfine splitting is just resolvable when the observed resonance is scanned more slowly with a smaller modulation amplitude. The other three resonances belong to "impurity" species and have not yet been assigned. The two signals marked B appear to be associated with each other.

molecular parameters employed are not quite accurate. Fortunately, reasonably reliable values for the molecular parameters of HF^+ were available from previous workers [6,8]. The resultant assignments are also given in Table 2. The quantum numbers used to describe the molecular states are J, Ω, parity, M_J, M_{I_1} and M_{I_2}, where I_1 and I_2 refer to the ^{19}F and ^1H nuclei, respectively. The nuclear spin de-coupled description is the appropriate one for experiments performed in a magnetic field. An estimate of the experimental uncertainty of each observation is given in the Table. Normally, we would expect this uncertainty to be dominated by the accuracy of the far-infrared laser frequencies which are re-settable to $\sqrt{2} \times 5 \times 10^{-7} \nu_L$. However, the modeling of the data with an effective Hamiltonian (see below) did not support this estimate; it seemed to underestimate the reliability of the higher frequency spectra. We have therefore given each measurement an uncertainty of 2 MHz instead.

3.2. Determination of molecular parameters

A nearly complete set of molecular parameters for $H^{19}F^+$ in the $v = 0$ level of its $X^2\Pi$ state was determined by fitting a model Hamiltonian to the present measurements by least-squares methods. The effective Hamiltonian was cast in the N^2 form as described by Brown et al. [22] with the Zeeman terms as described in [23]. The eigenstates were identified in terms of the Hund's case (a) quantum numbers given above. The basis set was truncated at states with $\Delta J = \pm 2$ which reproduced the exact calculations to within a few kHz for the highest field resonances. Each datum was weighted in the fit inversely as the square of its experimental error, estimated to be 2 MHz as given in Table 2. The parameter A_D was constrained to zero in the fit as a result of which the parameters A_D and γ are effective parameters [24].

The result of the least-squares fit is given in Table 2; the parameters determined in the process are given in Table 3 in both MHz and cm^{-1} units. Some of the smaller parameters ($H, q_D, g_l', g_r^{e'}$) have been constrained to values estimated from other sources, using the following relationships [23,25,26]:

$$H_0 \approx H_e = (2/3)D_e\{12(B_e/\omega_e)^2 - \alpha_e/\omega_e\}, \quad (1)$$

$$q_D = -(4D/B)q, \quad (2)$$

$$g_l' = p/2B, \quad (3)$$

$$g_r^{e'} = -q/B. \quad (4)$$

The values adopted are given in Table 3. In addition, the electron spin g-factor was fixed to a value of 2.0020, which corresponds to a relativistic correction of 1.5×10^{-4}. It can be seen from Table 2 that the ^1H hyperfine splittings were not resolved for most of the fine-structure transitions; consequently, there is very little information on the proton hyperfine interaction for the $^2\Pi_{1/2}$ levels. It was therefore only possible to determine one of the four proton hyperfine parameters in the fit,

Table 2
Observations in the far-infrared LMR spectrum of the HF^+ radical in the $v = 0$ level of the $X^2\Pi$ state

$J' \leftarrow J''$	$\Omega' \leftarrow \Omega''$	Parity	$M_J' \leftarrow M_J''$	M_{I_1}[a]	M_{I_2}[a]	B_0 (mT)	$\nu_L - \nu_{calc}$ (MHz)	$\partial\nu/\partial B_0$ (MHz/mT)	Uncert. (MHz)
124.4 μm spectrum $\nu_L = 2409293.3$ MHz									
$5/2 \leftarrow 3/2$	3/2	$+ \leftarrow -$	$1/2 \leftarrow 3/2$	1/2	1/2	1173.26	−1.01	−15.3	2.0
					−1/2	1176.15	−0.17	−15.3	2.0
				−1/2	1/2	1295.19	4.24	−15.4	2.0
					−1/2	1298.08	5.26	−15.4	2.0
		$- \leftarrow +$	$1/2 \leftarrow 3/2$	1/2	1/2	1361.80	−0.68	−15.3	2.0
					−1/2	1364.59	−1.49	−15.3	2.0
				−1/2	1/2	1484.42	−2.69	−15.4	2.0
					−1/2	1487.21	−3.34	−15.4	2.0
122.5 μm spectrum $\nu_L = 2447968.5$ MHz									
$5/2 \leftarrow 3/2$	3/2	$- \leftarrow +$	$-1/2 \leftarrow -3/2$	1/2	1/2	1024.90	−3.63	15.5	2.0
					−1/2	1027.70	−2.81	15.5	2.0
				−1/2	1/2	1129.84	0.97	15.4	2.0
					−1/2	1132.93	−2.46	15.4	2.0
		$+ \leftarrow -$	$-1/2 \leftarrow -3/2$	1/2	1/2	1209.49	0.46	15.5	2.0
					−1/2	1212.38	−0.27	15.5	2.0
				−1/2	1/2	1316.13	3.65	15.4	2.0
					−1/2	1319.02	3.07	15.4	2.0
		$- \leftarrow +$	$1/2 \leftarrow -1/2$	1/2	1/2	1750.00	0.31	9.34	2.0
					−1/2	1752.40	0.69	9.34	2.0
87.73 μm spectrum $\nu_L = 3417.2639$ MHz									
$7/2 \leftarrow 5/2$	3/2	$+ \leftarrow -$	$-3/2 \leftarrow -5/2$	1/2	1/2	1227.75	0.80	9.28	2.0
					−1/2	1230.04	1.70	9.28	2.0
				−1/2	1/2	1324.91	1.07	9.19	2.0
					−1/2	1327.30	1.21	9.19	2.0
		$+ \leftarrow -$	$-1/2 \leftarrow -3/2$	1/2	1/2	1612.34	2.05	7.10	2.0
					−1/2	1614.62	0.78	7.10	2.0
				−1/2	1/2	1714.07	0.73	7.07	2.0
					−1/2	1716.41	−0.86	7.07	2.0
		$- \leftarrow +$	$-3/2 \leftarrow -5/2$	1/2	1/2	1810.60	−2.70	9.29	2.0
					−1/2	1812.90	−2.07	9.29	2.0
				−1/2	1/2	1911.90	−1.11	9.25	2.0
					−1/2	1914.33	−1.63	9.25	2.0
48.72 μm spectrum $\nu_L = 6153.2790$ MHz									
$7/2 \leftarrow 9/2$	$1/2 \leftarrow 3/2$	$- \leftarrow +$	$-3/2 \leftarrow -3/2$	1/2	[b]	233.43	−1.01	5.23	2.0
			$-5/2 \leftarrow -5/2$	−1/2	[b]	411.14	1.04	10.50	2.0
			$-3/2 \leftarrow -3/2$	−1/2	[b]	650.59	1.24	6.48	2.0
			$-7/2 \leftarrow -9/2$		[b]	65.18	0.32	16.89	2.0
			$-5/2 \leftarrow -7/2$	1/2	[b]	88.76	−0.40	12.51	2.0
			$-7/2 \leftarrow -9/2$		[b]	254.52	−1.04	17.26	2.0
			$-3/2 \leftarrow -5/2$	−1/2	[b]	457.60	1.21	9.40	2.0
			$-1/2 \leftarrow -3/2$		[b]	780.40	−1.44	5.35	2.0
44.24 μm spectrum $\nu_L = 6775783.5$ MHz									
$5/2 \leftarrow 7/2$	$1/2 \leftarrow 3/2$	$+ \leftarrow -$	$-5/2 \leftarrow -5/2$	1/2	[b]	424.33	−1.60	12.37	2.0
				−1/2	[b]	658.99	−3.57	12.78	2.0
			$-3/2 \leftarrow -3/2$	1/2	[b]	749.72	−0.82	7.29	2.0
				−1/2	[b]	1057.26	3.38	7.80	2.0
		$+ \leftarrow -$	$-5/2 \leftarrow -7/2$	−1/2	[b]	316.29	2.98	16.32	2.0
		$- \leftarrow +$	$5/2 \leftarrow 5/2$	−1/2	−1/2	1951.53	−1.37	−12.50	[c]
					1/2	1953.48	−9.15	−12.50	[c]
		$+ \leftarrow -$		1/2	[b]	510.97	0.30	16.61	2.0
		$- \leftarrow +$	$5/2 \leftarrow 7/2$	−1/2	−1/2	1504.46	−3.59	−16.35	2.0
					1/2	1506.55	2.53	−16.35	2.0
				1/2	−1/2	1608.38	−0.90	−16.47	2.0
					1/2	1610.30	1.47	−16.47	2.0
39.92 μm spectrum $\nu_L = 7509036.2$ MHz									
$3/2 \leftarrow 5/2$	$1/2 \leftarrow 3/2$	$+ \leftarrow -$	$-3/2 \leftarrow -3/2$	$1/2 \leftarrow -1/2$	[b]	69.67	−1.68	6.18	2.0
			$-3/2 \leftarrow -5/2$	1/2	[b]	150.84	−0.47	15.92	2.0
			$-1/2 \leftarrow -3/2$	1/2	[b]	301.00	1.98	8.42	2.0

Table 2 (*continued*)

$J' \leftarrow J''$	$\Omega' \leftarrow \Omega''$	Parity	$M_J' \leftarrow M_J''$	M_{I_1} [a]	M_{I_2} [a]	B_0 (mT)	$\nu_L - \nu_{calc}$ (MHz)	$\partial\nu/\partial B_0$ (MHz/mT)	Uncert. (MHz)
		+ ← −	−3/2 ← −3/2	1/2 ← −1/2	[b]	397.54	0.75	10.56	2.0
		− ← +	−3/2 ← −5/2	1/2	[b]	1525.09	−0.01	16.64	2.0
				−1/2	[b]	1702.29	−0.86	16.75	2.0

[a] I_1 and I_2 are the nuclear spins of the ^{19}F and ^{1}H nuclei, respectively. Transitions obey the allowed nuclear spin selection rule $\Delta M_{I_1} = \Delta M_{I_2} = 0$ unless indicated.

[b] ^{1}H hyperfine splitting not resolved.

[c] Lines excluded from the least-squares fit because their flux densities were beyond the calibrated range.

Table 3
Molecular parameters for HF^+ in the $v = 0$ level of the $X^2\Pi$ state

Parameter	Value (MHz)	Value (cm^{-1})
$\tilde{A} + \tilde{\gamma}$	−8736638 (17)[a]	−291.422 90 (57)
$\tilde{\gamma}$	−8258 (32)	−0.2754 (11)
$\tilde{\gamma}_D$	2.40 (66)	$0.80\ (22) \times 10^{-4}$
B	513219.5 (23)	17.119160 (78)
D	66.806 (63)	$0.22284\ (21) \times 10^{-2}$
H	0.4905×10^{-2}[b]	0.1636×10^{-6}[b]
$p + 2q$	15418.4 (52)	0.51430 (17)
$p_D + 2q_D$	−1.82 (47)	$-0.61(16) \times 10^{-4}$
q	−1200.60 (39)	$-0.40048\ (13) \times 10^{-1}$
q_D	0.340[b]	0.113×10^{-4}[b]
$h_{1/2}$ (F)	4626 (16)	0.15430 (52)
$h_{3/2}$ (F)	3345.8 (22)	0.111605 (75)
b (F)	1301.0 (92)	$0.4340\ (31) \times 10^{-1}$
d (F)	5167.3 (50)	0.17236 (17)
$h_{1/2}$ (H)	70.24[b]	0.2343×10^{-2}[b]
$h_{3/2}$ (H)	93.7 (19)	$0.3126\ (65) \times 10^{-2}$
b (H)	−103.58[b]	-0.3455×10^{-2}[b]
d (H)	50.24[b]	0.1676×10^{-2}[b]
g_L'	1.00118 (23)	
g_S	2.0020[b]	
g_l	$0.90\ (31) \times 10^{-2}$	
g_r	$-0.57\ (15) \times 10^{-3}$	
$g_l' - g_r^{e'}$	0.1502×10^{-1}[b]	
$g_r^{e'}$	0.2339×10^{-2}[b]	
g_N (F)	5.257731[c]	
g_N (H)	5.585690[c]	

[a] Numbers in parentheses are one standard deviation of the least-squares fit, in units of the last quoted decimal place.

[b] Parameter constrained to this value in the fit (see text).

[c] Nuclear spin g-factors in nuclear magnetons.

namely $h_{3/2}$ which governs the splittings in the levels of the $^2\Pi_{3/2}$ component. The values for the other three parameters were constrained to values estimated from those for the corresponding parameters of ^{16}OH [27,28]. The estimates were obtained by scaling as $1/r^3$ where r is the bond length of the molecule (approximately the separation of the unpaired electron from the ^{1}H nucleus). Using these constrained values, the standard deviation of the fit of 55 data points relative to experimental uncertainties is 1.187, a figure which can be regarded as entirely satisfactory (a value of 1.0 is expected if the model is adequate and the weighting factors have been chosen correctly).

4. Discussion

Although the measurements of the far-infrared LMR spectrum of HF^+ in the $v = 0$ level of its $X^2\Pi$ state are not very extensive, they have allowed the determination of an essentially complete set of molecular parameters in the effective Hamiltonian, including the ^{19}F hyperfine parameters. The values determined are also significantly more accurate than those obtained previously by optical spectroscopy [6] and by a combination of far-infrared LMR and infrared spectroscopy [8], as shown in Tables 4 and 5. Using our values for the ground state parameters and the value for $\gamma_e(= \beta_B)$ of $0.0142\,cm^{-1}$ determined by Gewurtz et al. [6], we have re-fit the infrared measurements of Hovde et al. [8] to determine a value for $\alpha_e(= -\alpha_B)$ of $0.88441(16)\,cm^{-1}$. This can be combined with our value for B_0 to determine the value for the rotational constant at equilibrium, $B_e = 17.55782\ (11)\,cm^{-1}$. This in turn corresponds to a value for r_e of 1.0016005 (32) Å where the quoted error is purely statistical. This equilibrium bond length is significantly longer than that of HF in its ground $^1\Sigma^+$ state (0.91681 Å [29]). The lambda-doubling parameters are also much better determined, particularly the combination $(p + 2q)$ which governs the doubling in the $^2\Pi_{1/2}$ component; the present study gives values for p and q of 0.5944 and $-0.04005\,cm^{-1}$ respectively. Hutson and Cooper [12] have made an accurate ab initio calculation of these parameters; for comparison, their values for p and q for the zero-point vibrational level were 0.589 and $-0.0402\,cm^{-1}$, respectively. An important feature of their calculation was the inclusion of the effect of the continuum of vibrational levels above the weakly bound $A^2\Sigma^+$ state.

Perhaps the most interesting numbers are the values for the ^{19}F hyperfine parameters which have been assembled in Table 5. They clearly represent a marked improvement over the previous determination which was very much at the limit of the experimental method [8] despite the large size of the interaction. Of the four values, only those for $h_{3/2}$(F) are in reasonably good agreement with the earlier work; this is because they are derived from LMR measurements on HF^+ in the $^2\Pi_{3/2}$ levels in both studies. The same remark might be ex-

Table 4
Comparison of molecular parameters determined for HF^+ in the $v = 0$ level of the $X^2\Pi$ state

Parameter[a]	Present work	Optical study[b]	Previous LMR & IR[c]
B_0	17.119168 (78)	17.1375 (25)	17.11429(31)
D_0	0.22284 (21) × 10^{-2}	0.2205 (14) × 10^{-2}	0.22085 (40) × 10^{-2}
$\tilde{A}_0 + \tilde{\gamma}_0$	−291.42290 (57)	−292.541 (17)	−291.418 (14)
$\tilde{\gamma}_0$	−0.2754 (11)	[d]	−0.2704 (44)[e]
$p_0 + 2q_0$	0.51430 (17)	0.548 (60) × 10^{-1}	0.51704 (254)
q_0	−0.40048 (13) × 10^{-1}	−0.46 (8) × 10^{-1}	−0.4054 (11) × 10^{-1}

[a] Values given in cm^{-1}.
[b] Values determined by Gewurtz et al. [6] from an analysis of the $A^2\Sigma^+$–$^2\Pi$ electronic spectrum.
[c] Values determined by Hovde et al. [8] from an analysis of the FIR LMR and IR spectra.
[d] Parameter not determined [13].
[e] The value for γ_0 has been calculated from that given for A_D (−0.02842 cm^{-1}) by Hovde et al. [8].

Table 5
Comparison of nuclear hyperfine parameters for HF^+ in the $v = 0$ level of the $X^2\Pi$ state

Parameter[a]	Present work	Previous LMR & IR[b]
$h_{1/2}$ (F)	4626 (16)	5500 (1800)
$h_{3/2}$ (F)	3345.8 (22)	3354 (14)
b (F)	1301.0 (92)	1270 (140)
d (F)	5167.3 (50)	4900 (1000)
$h_{3/2}$ (H)	93.7 (19)	83.2 (44)

[a] Values given in MHz.
[b] Values determined by Hovde et al. [8] from an analysis of the FIR LMR and IR spectra.

pected to apply to the corresponding parameter for the ^1H nucleus, $h_{3/2}$(H), but in this case the agreement is not so good. This possibly reflects the values to which the other hyperfine parameters were constrained in the fit. We have estimated the values by scaling from those for the OH radical, a procedure which is only moderately vindicated by the value for $h_{3/2}$(H) determined (the value expected was 82.58 MHz). Hovde et al. [8] appear to have constrained these other parameters to zero.

The first full determination of the ^{19}F hyperfine parameters in HF^+ provides information about the distribution of the open-shell electron(s) in this molecule. The various expectation values [30] and their experimentally derived values are given in Table 6. In this table, they are compared with the values calculated ab initio by Kristiansen and Veseth [13] and with the corresponding values calculated for the atomic ion F^+ [31].

Table 6
Interpretation of ^{19}F nuclear hyperfine parameters for HF^+ in the $v = 0$ level of the $X^2\Pi$ state

Parameter[a]	Present work	Ab initio calculation[b]	Value for F^+[c]
$\langle 1/r_i^3 \rangle_l$	7.9455	7.8898	8.4088
$\langle \delta(r_i) \rangle_s$	0.10474	0.136	0.09356
$\langle (3\cos^2\theta_i - 1)/r_i^3 \rangle_s$	−3.4261	−3.3146	...
$\langle \sin^2\theta_i/r_i^3 \rangle_s$	6.8593	6.8097	...
$\langle 1/r_i^3 \rangle_s$	8.5758	...	9.1178

[a] Values given in au^{-3}.
[b] Values determined by Kristiansen and Veseth [13].
[c] Values determined by Schaeffer and Klemm [31].

It can be seen that the values of Kristiansen and Veseth are remarkably good (with the slight exception of the spin density at the ^{19}F nucleus which is notoriously difficult to calculate reliably). The expectation values for F^+ are also close to those for HF^+, consistent with a description of an open-shell electronic wavefunction which is confined largely to the F atom. In their experimental study of the fine-structure spectrum of F^+, Brown et al. [15] suggest that the value for $\langle \delta(r_i) \rangle_s$ should be raised to 0.170 (55) au, which would then be slightly larger than the value determined for HF^+.

As can be seen in Table 3, we have been able to determine three of the six possible g-factors for a molecule in a $^2\Pi$ state. The orbital g-factor g'_L deviates from unity because of relativistic and non-adiabatic corrections [32]. The former is typically about -1.5×10^{-4}, from which the non-adiabatic correction, Δg_L, is calculated to be 1.33 (23) × 10^{-3}. The rotational g-factor g_r has nuclear and electronic contributions:

$$g_r = g_r^N - g_r^e. \tag{5}$$

The nuclear contribution depends only on the nuclear masses and charges for a diatomic molecule [30]; for $H^{19}F^+$, it is calculated to be 0.5300 × 10^{-3} (in units of Bohr magnetons) leaving g_r^e as 1.10 (15) × 10^{-3}. The two parameters Δg_L and g_r^e have essentially the same physical origin in the effective Hamiltonian, both depending on the admixture of $^2\Sigma$ and $^2\Delta$ states [32]. However, while Δg_L depends on the difference of these two effects, g_r^e depends on their sum. Thus if a $^2\Pi$ state is contaminated by $^2\Sigma$ states alone, Δg_L is equal to g_r^e. Our experimental result shows that this is the case, to within experimental error, and we thus have evidence that the $X^2\Pi$ state of HF^+ is contaminated predominantly by $^2\Sigma$ states. The other g-factor determined in our fit is g_l, the anisotropic correction to the electron spin magnetic moment. Though the value in Table 3 (0.90 (31) × 10^{-2}) is not very precisely determined, it agrees reasonably well with the expectations of Curl's relationship [33], $-\gamma/2B$ or 0.805 × 10^{-2}. However, it should be remembered that γ is an effective parameter in our fit, containing a contribution from the parameter A_D also [24].

Table 7
Calculated rotational and fine-structure transition frequencies of the HF^+ radical in the $v = 0$ level of the $X^2\Pi$ state

$\Omega' \leftarrow \Omega''$	$J' \leftarrow J''$	Parity	$F_1' \leftarrow F_1''$[a]	ν (MHz)	Vacuum wavelength (μm)	Linestrength[b] $S_{F'F}$
3/2	5/2 ← 3/2	− ← +	2 ← 1	2431879.4(30)[c]	123.27604	1.2028
			2 ← 2	2429084.7(30)	123.41787	0.1340
			3 ← 2	2431019.7(30)	123.31963	1.8725
		+ ← −	2 ← 1	2429028.9(30)	123.42070	1.2029
			2 ← 2	2426278.9(30)	123.56059	0.1339
			3 ← 2	2428103.9(30)	123.46772	1.8725
	7/2 ← 5/2	− ← +	3 ← 2	3400322.9(30)	88.16588	2.3876
			3 ← 3	3398497.9(30)	88.21322	0.1195
			4 ← 3	3399890.1(30)	88.17710	3.2241
		+ ← −	3 ← 2	3405711.0(30)	88.02640	2.3876
			3 ← 3	3403775.9(30)	88.07644	0.1195
			4 ← 3	3405361.0(30)	88.03544	3.2240
	9/2 ← 7/2[d]	− ← +	4 ← 3	4379936.4(45)	68.44676	3.5101
			4 ← 4	4378351.4(45)	68.47154	0.1004
			5 ← 4	4379770.3(45)	68.44936	4.4132
		+ ← −	4 ← 3	4371584.1(45)	68.57753	3.5103
			4 ← 4	4370191.9(45)	68.59938	0.1003
			5 ← 4	4371323.6(45)	68.58162	4.4134
1/2	3/2 ← 1/2[d]	− ← +	1 ← 0	1612974.5(60)	185.86311	0.6606
			1 ← 1	1613342.7(60)	185.82069	0.3302
			2 ← 1	1611741.0(60)	186.00536	1.6539
		+ ← −	1 ← 0	1629134.5(60)	184.01946	0.6593
			1 ← 1	1622606.4(60)	184.75981	0.3323
			2 ← 1	1626469.6(60)	184.32097	1.6534
	5/2 ← 3/2[d]	− ← +	2 ← 1	2699792.5(60)	111.04278	1.4858
			2 ← 2	2695929.3(60)	111.20190	0.1990
			3 ← 2	2699159.2(60)	111.06883	2.7786
		+ ← −	2 ← 1	2686906.5(60)	111.57532	1.7856
			2 ← 2	2688508.2(60)	111.50885	0.1981
			3 ← 2	2686534.2(60)	111.59078	2.7784
1/2	7/2 ← 5/2[d]	− ← +	3 ← 2	3753095.4(40)	79.87872	2.8361
			3 ← 3	3755069.4(40)	79.83673	0.1417
			4 ← 3	3752910.4(40)	79.88266	3.8290
		+ ← −	3 ← 2	3763227.7(40)	79.66365	2.8365
			3 ← 3	3759997.8(40)	79.73208	0.1420
			4 ← 3	3762894.6(40)	79.67070	3.8298
1/2 ← 3/2	3/2 ← 3/2[d]	− ← +	1 ← 1	9913114.9(80)	30.24200	0.118×10^{-3}
			1 ← 2	9910364.9(80)	30.25040	0.235×10^{-4}
			2 ← 1	9911513.2(80)	30.24689	0.236×10^{-4}
			2 ← 2	9908763.2(80)	30.25529	0.212×10^{-3}
		+ ← −	1 ← 1	9938545.5(80)	30.16462	0.118×10^{-3}
			1 ← 2	9935750.8(80)	30.17311	0.240×10^{-4}
			2 ← 1	9942408.6(80)	30.15290	0.237×10^{-4}
			2 ← 2	9939614.0(80)	30.16138	0.213×10^{-3}
	5/2 ← 5/2[d]	− ← +	2 ← 2	10206458.6(80)	29.37282	0.239×10^{-3}
			2 ← 3	10204523.6(80)	29.37839	0.173×10^{-4}
			3 ← 2	10209688.5(80)	29.36353	0.171×10^{-4}
			3 ← 3	10207753.4(80)	29.36909	0.342×10^{-3}
		+ ← −	2 ← 2	10170992.5(80)	29.47524	0.238×10^{-3}
			2 ← 3	10169167.5(80)	29.48053	0.170×10^{-4}
			3 ← 2	10169018.6(80)	29.48096	0.170×10^{-4}
			3 ← 3	10167193.5(80)	29.48625	0.340×10^{-3}
1/2 ← 3/2	1/2 ← 3/2[d]	− ← +	0 ← 1	8310387.8(80)	36.07442	0.171×10^{-3}
			1 ← 1	8316916.0(80)	36.04611	0.856×10^{-4}
			1 ← 2	8314165.9(80)	36.05803	0.427×10^{-4}
		+ ← −	0 ← 1	8299163.5(80)	36.12321	0.171×10^{-3}
			1 ← 1	8298795.3(80)	36.12482	0.859×10^{-4}
			1 ← 2	8296000.7(80)	36.13699	0.427×10^{-4}
	3/2 ← 5/2	− ← +	1 ← 2	7480258.7(60)	40.07782	0.372×10^{-3}
			2 ← 2	7478657.0(60)	40.08640	0.415×10^{-4}
			2 ← 3	7476722.0(60)	40.09678	0.578×10^{-4}
		+ ← −	1 ← 2	7510493.4(60)	39.91648	0.371×10^{-3}
			2 ← 2	7514356.6(60)	39.89596	0.412×10^{-4}

Table 7 (*continued*)

$\Omega' \leftarrow \Omega''$	$J' \leftarrow J''$	Parity	$F_1' \leftarrow F_1''$[a]	ν (MHz)	Vacuum wavelength (μm)	Linestrength[b] $S_{F'F}$
			$2 \leftarrow 3$	7512531.6(60)	39.90565	0.577×10^{-4}
$1/2 \leftarrow 3/2$	$5/2 \leftarrow 7/2$	$- \leftarrow +$	$2 \leftarrow 3$	6809963.0(60)	44.02263	0.577×10^{-3}
			$3 \leftarrow 3$	6813192.8(60)	44.00176	0.288×10^{-4}
			$3 \leftarrow 4$	6811800.6(60)	44.01075	0.779×10^{-4}
		$+ \leftarrow -$	$2 \leftarrow 3$	6761454.2(60)	44.33846	0.579×10^{-3}
			$3 \leftarrow 3$	6759480.3(60)	44.35141	0.291×10^{-4}
			$3 \leftarrow 4$	6757895.2(60)	44.36181	0.782×10^{-4}
	$7/2 \leftarrow 9/2$	$- \leftarrow +$	$3 \leftarrow 4$	6134613.2(60)	48.86901	0.817×10^{-3}
			$4 \leftarrow 4$	6132454.2(60)	48.88621	0.234×10^{-4}
			$4 \leftarrow 5$	6131035.3(60)	48.89753	0.103×10^{-2}
		$+ \leftarrow -$	$3 \leftarrow 4$	6201606.5(60)	48.34110	0.811×10^{-3}
			$4 \leftarrow 4$	6204503.3(60)	48.31853	0.232×10^{-4}
			$4 \leftarrow 5$	6203371.7(60)	48.32734	0.102×10^{-2}
	$9/2 \leftarrow 11/2$[d]	$- \leftarrow +$	$4 \leftarrow 5$	5675602.7(80)	52.82126	0.107×10^{-2}
			$5 \leftarrow 5$	5678270.8(80)	52.79644	0.199×10^{-4}
			$5 \leftarrow 6$	5677320.1(80)	52.80528	0.129×10^{-2}
		$+ \leftarrow -$	$4 \leftarrow 5$	5590006.9(80)	53.63007	0.811×10^{-2}
			$5 \leftarrow 5$	5587743.2(80)	53.65180	0.201×10^{-4}
			$5 \leftarrow 6$	5586404.7(80)	53.66465	0.131×10^{-2}

[a] Coupling scheme: $\boldsymbol{J} = \boldsymbol{N} + \boldsymbol{S}$; $\boldsymbol{F_1} = \boldsymbol{J} + \boldsymbol{I}_1$; $\boldsymbol{F} = \boldsymbol{F_1} + \boldsymbol{I}_2$, where $\boldsymbol{I}_1$ and $\boldsymbol{I}_2$ are the ^{19}F and ^{1}H nuclear spins respectively. The proton hyperfine splittings are not included.

[b] For definition, see Eq. (6).

[c] Estimated uncertainty in units of the last quoted decimal place (1σ).

[d] Transition not directly studied in the LMR experiment.

We have used the values for the molecular parameters in Table 3 to calculate the zero-field rotational spectrum of HF^+. The computed values of the transition frequencies for levels up to $J = 9/2$ are given in Table 7. For the sake of simplicity, the relatively small proton hyperfine splittings have not been included. The computed linestrengths $S_{F'F}$, which are also listed in Table 7, can be used to assess the relative intensities of individual transitions. The linestrength is defined by

$$S_{F'F} = |\langle \gamma' F' \| D^{(1)}_{.q}(\omega)^* \| \gamma F \rangle|^2, \tag{6}$$

where the quantity on the right-hand side is the reduced matrix element of the rotation matrix [34] and γ stands for subsidiary quantum numbers. The intensity of the line in absorption can be obtained by multiplying the linestrength by the square of the dipole moment μ, by the transition frequency and by the population difference between the lower and upper states. The Einstein A-coefficients for spontaneous emission from state i to j can also be calculated from the linestrengths by use of the relation

$$A_{i \to j} = (16\pi^3 \nu_{ij}^3 / 3\varepsilon_0 hc^3)(2F_i + 1)^{-1} S_{ij} \mu^2. \tag{7}$$

Table 7 is not quite complete because the fine-structure transitions with $\Delta J = 1$ (R-lines) have been omitted. These transitions are very weak and occur at considerably higher frequencies (at wavelengths shorter than 25 μm).

This paper describes a study of the far-infrared LMR spectrum of the HF^+ radical which is incomplete. The work was curtailed prematurely by the unexpected illness and death of Ken Evenson in 2002. It was in fact the last piece of experimental work to be carried out in his laboratory at Boulder before it was closed down. Consequently, much remains to be done on this interesting molecule. Several other coincidences with short-wave laser lines await investigation. It might also be possible to study some transitions in the $^2\Pi_{1/2}$ manifold despite their slow tunability since there are suitable laser lines very close in frequency. Finally, it could well be that HF^+ is sufficiently energized in the microwave discharge that it would be possible to study its spectrum in excited vibrational levels.

Acknowledgments

MDA is grateful for the support of a NRC Post-doctoral Fellowship. This study was supported in part by NASA contract W15,047.

References

[1] D.C. Frost, C.A. McDowell, D.A. Vroom, J. Chem. Phys. 46 (1967) 4255–4259.
[2] C.R. Brundle, Chem. Phys. Lett. 7 (1970) 317–322.
[3] J. Berkowitz, W.A. Chupka, P.M. Guyon, J.H. Holloway, R. Spohr, J. Chem. Phys. 54 (1971) 5165–5180.
[4] J. Berkowitz, Chem. Phys. Lett. 11 (1971) 21–26.
[5] P.M. Guyon, R. Spohr, W.W. Chupka, J. Berkowitz, J. Chem. Phys. 65 (1976) 1650–1658.
[6] S. Gewurtz, H. Lew, P. Flainek, Can. J. Phys. 53 (1975) 1097–1108.

[7] D.C. Hovde, E. Schäfer, S.E. Strahan, C.A. Ferrari, D. Ray, K.G. Lubic, R.J. Saykally, Mol. Phys. 52 (1984) 245–249.
[8] D.C. Hovde, E.R. Keim, R.J. Saykally, Mol. Phys. 68 (1989) 599–607.
[9] P.S. Julienne, M. Krauss, A.C. Wahl, Chem. Phys. Lett. 11 (1971) 16–20.
[10] P. Rosmus, W. Meyer, J. Chem. Phys. 66 (1977) 13–19.
[11] I.D.L. Wilson, J. Mol. Spectrosc. 70 (1978) 394–404.
[12] J.M. Hutson, D.L. Cooper, J. Chem. Phys. 75 (1981) 4502–4506.
[13] P. Kristiansen, L. Veseth, J. Chem. Phys. 84 (1986) 6336–6344.
[14] H. Odashima, L.R. Zink, K.M. Evenson, J. Mol. Spectrosc. 194 (1999) 283–284.
[15] J.M. Brown, L.R. Zink, K.M. Evenson, Phys. Rev. A 57 (1998) 2507–2510.
[16] F. Tamassia, J.M. Brown, K.M. Evenson, J. Chem. Phys. 110 (1999) 7273–7286.
[17] H. Körsgen, K.M. Evenson, J.M. Brown, J. Chem. Phys. 107 (1997) 1025–1027.
[18] T.J. Sears, P.R. Bunker, A.R.W. McKellar, K.M. Evenson, D.A. Jennings, J.M. Brown, J. Chem. Phys. 77 (1982) 5348–5362.
[19] T.D. Varberg, J.M. Brown, K.M. Evenson, J. Chem. Phys. 100 (1994) 2487–2491.
[20] J.M. Brown, C.M.L. Kerr, F.D. Wayne, K.M. Evenson, H.E. Radford, J. Mol. Spectrosc. 86 (1981) 544–554.
[21] J.M. Brown, K.M. Evenson, J. Mol. Spectrosc. 98 (1983) 392–403.
[22] J.M. Brown, E.A. Colbourn, J.K.G. Watson, F.D. Wayne, J. Mol. Spectrosc. 74 (1979) 294–318.
[23] J.M. Brown, M. Kaise, C.M.L. Kerr, D.J. Milton, Mol. Phys. 36 (1978) 553–583.
[24] J.M. Brown, J.K.G. Watson, J. Mol. Spectrosc. 65 (1977) 65–74.
[25] G. Herzberg, Spectra of Diatomic Molecules, Van Nostrand, Princeton, NJ, 1950.
[26] L. Veseth, J. Phys. B. 3 (1970) 1677–1691.
[27] W.L. Meerts, A. Dymanus, Can. J. Phys. 53 (1975) 2123–2141.
[28] W.L. Meerts, Chem. Phys. Lett. 46 (1977) 24–28.
[29] K.-P. Huber, G. Herzberg, Constants of Diatomic Molecules, Van Nostrand Reinhold, New York, 1979.
[30] J.M. Brown, A. Carrington, Rotational Spectroscopy of Diatomic Molecules, Cambridge University Press, Cambridge, 2003.
[31] H.F. Schaeffer III, R.A. Klemm, Phys. Rev. A 1 (1970) 1063–1069.
[32] J.M. Brown, H. Uehara, Mol. Phys. 24 (1972) 1169–1174.
[33] R.F. Curl Jr., Mol. Phys. 9 (1965) 585–597.
[34] D.M. Brink, G.R. Satchler, Angular Momentum, third ed., Oxford University Press, Oxford, 1993.

Available online at www.sciencedirect.com
SCIENCE DIRECT®
Journal of Molecular Spectroscopy 227 (2004) 23–27
Journal of MOLECULAR SPECTROSCOPY
www.elsevier.com/locate/jms

Millimeter-wave spectrum of BrCN produced by dc discharge

Pradeep Risikrishna Varadwaj and A.I. Jaman*

Saha Institute of Nuclear Physics, 1/AF Bidhannagar, Kolkata 700 064, India

Received 22 October 2003; in revised form 7 May 2004
Available online 8 June 2004

Abstract

Ground state ($v = 0$) and first excited state ($v = 1$) millimeter-wave rotational absorption spectra of cyanogen bromide (BrCN) and some of its isotopic species, have been investigated in the frequency region: 40.0–75.0 GHz using a source-modulated millimeter-wave spectrometer. Millimeter-wave radiation has been produced using a frequency multiplier, the fundamental radiation source being klystrons. BrCN has been produced by applying a dc glow discharge through a mixture of 3-bromobenzonitrile and trifluoromethylbromide (CF_3Br) at low pressure. The quadrupole hyperfine structure of ^{81}Br and ^{79}Br have been resolved, measured, and analyzed. Finally, internuclear distances of BrCN have been determined.

Keywords: Millimeter-wave spectroscopy; Cyanogen bromide (BrCN); Discharges; Molecular structure

1. Introduction

Production of molecules by dc glow discharge has proved to be a very important and useful technique. This technique appears to be highly suitable for the generation of transient species which are difficult to synthesize by ordinary chemical methods. Cyanogen fluoride FCN [1] and many halogen derivatives of acetylenic compound HCCF [2], HCCCCF [3], ClCCF [4], BrCCF [5], FCCCN [6], etc. have been produced by dc glow discharge and were characterized by various spectroscopic methods. However, the production of cyanogen bromide (BrCN) using dc glow discharge method has not yet been reported. Analysis of pure rotational transitions of BrCN ($J = 2 \rightarrow 3$) was first reported by Townes et al. [7]. Subsequently, Bardeen and Townes [8] have analysed the quadrupole hyperfine structure of the Br nucleus. Later on, the $J = 3 \rightarrow 4$ rotational transitions of BrCN have been observed and analyzed by Gordy et al. [9,10]. The rotational analysis has been extended to the millimeter-wave region by Burrus et al. [11] and to the millimeter-wave and submillimeter-wave region by Le Guennec et al. [12] who have reported only the quadrupole free line centers. The microwave spectrum for $J = 0 \rightarrow 1$ and $J = 1 \rightarrow 2$ of BrCN have been reported by Cogley et al. [13]. Millimeter-wave spectra of ^{15}N species of BrCN has been analysed by Tamassia et al. [14] in the ground and in some low-lying excited vibrational states. However, in all the previous works, BrCN was either procured commercially or prepared chemically.

In the present communication, we report the analysis of millimeter-wave rotational spectra and Br nuclear quadrupole hyperfine structure of BrCN and some of its isotopic species produced by a dc glow discharge of a low pressure mixture of 3-bromobenzonitrile and trifluoromethylbromide (CF_3Br). Intermediate J values ($J = 5$–9) are involved in this work covering the frequency range 40.0–75.0 GHz, where no hyperfine structural data is reported so far. The rotational, centrifugal distortion, and quadrupole coupling constant values were obtained from a least-squares analysis of the observed data. Finally, using the parent and isotopic species data Br–C and C–N bond lengths have been determined with the help of Kraitchman's equation and compared with previously reported values.

Analysis of the rotational spectrum of ClCN produced by dc glow discharge is underway and will be reported in a separate communication.

* Corresponding author. Fax: +91-33-2337-4637.
E-mail address: jaman@cmp.saha.ernet.in (A.I. Jaman).

0022-2852/$ - see front matter © 2004 Elsevier Inc. All rights reserved.
doi:10.1016/j.jms.2004.05.003

[7] D.C. Hovde, E. Schäfer, S.E. Strahan, C.A. Ferrari, D. Ray, K.G. Lubic, R.J. Saykally, Mol. Phys. 52 (1984) 245–249.
[8] D.C. Hovde, E.R. Keim, R.J. Saykally, Mol. Phys. 68 (1989) 599–607.
[9] P.S. Julienne, M. Krauss, A.C. Wahl, Chem. Phys. Lett. 11 (1971) 16–20.
[10] P. Rosmus, W. Meyer, J. Chem. Phys. 66 (1977) 13–19.
[11] I.D.L. Wilson, J. Mol. Spectrosc. 70 (1978) 394–404.
[12] J.M. Hutson, D.L. Cooper, J. Chem. Phys. 75 (1981) 4502–4506.
[13] P. Kristiansen, L. Veseth, J. Chem. Phys. 84 (1986) 6336–6344.
[14] H. Odashima, L.R. Zink, K.M. Evenson, J. Mol. Spectrosc. 194 (1999) 283–284.
[15] J.M. Brown, L.R. Zink, K.M. Evenson, Phys. Rev. A 57 (1998) 2507–2510.
[16] F. Tamassia, J.M. Brown, K.M. Evenson, J. Chem. Phys. 110 (1999) 7273–7286.
[17] H. Körsgen, K.M. Evenson, J.M. Brown, J. Chem. Phys. 107 (1997) 1025–1027.
[18] T.J. Sears, P.R. Bunker, A.R.W. McKellar, K.M. Evenson, D.A. Jennings, J.M. Brown, J. Chem. Phys. 77 (1982) 5348–5362.
[19] T.D. Varberg, J.M. Brown, K.M. Evenson, J. Chem. Phys. 100 (1994) 2487–2491.
[20] J.M. Brown, C.M.L. Kerr, F.D. Wayne, K.M. Evenson, H.E. Radford, J. Mol. Spectrosc. 86 (1981) 544–554.
[21] J.M. Brown, K.M. Evenson, J. Mol. Spectrosc. 98 (1983) 392–403.
[22] J.M. Brown, E.A. Colbourn, J.K.G. Watson, F.D. Wayne, J. Mol. Spectrosc. 74 (1979) 294–318.
[23] J.M. Brown, M. Kaise, C.M.L. Kerr, D.J. Milton, Mol. Phys. 36 (1978) 553–583.
[24] J.M. Brown, J.K.G. Watson, J. Mol. Spectrosc. 65 (1977) 65–74.
[25] G. Herzberg, Spectra of Diatomic Molecules, Van Nostrand, Princeton, NJ, 1950.
[26] L. Veseth, J. Phys. B. 3 (1970) 1677–1691.
[27] W.L. Meerts, A. Dymanus, Can. J. Phys. 53 (1975) 2123–2141.
[28] W.L. Meerts, Chem. Phys. Lett. 46 (1977) 24–28.
[29] K.-P. Huber, G. Herzberg, Constants of Diatomic Molecules, Van Nostrand Reinhold, New York, 1979.
[30] J.M. Brown, A. Carrington, Rotational Spectroscopy of Diatomic Molecules, Cambridge University Press, Cambridge, 2003.
[31] H.F. Schaeffer III, R.A. Klemm, Phys. Rev. A 1 (1970) 1063–1069.
[32] J.M. Brown, H. Uehara, Mol. Phys. 24 (1972) 1169–1174.
[33] R.F. Curl Jr., Mol. Phys. 9 (1965) 585–597.
[34] D.M. Brink, G.R. Satchler, Angular Momentum, third ed., Oxford University Press, Oxford, 1993.